

# Contrasting effects of lanthanum and samarium modifiers on the elastic and non-linear acoustic properties of phosphate glasses

H. B. SENIN, G. A. SAUNDERS, LI JIAQIANG, P. J. FORD  
*School of Physics, University of Bath, Claverton Down, Bath BA2 7AY, UK*

While samarium phosphate  $(\text{Sm}_2\text{O}_3)_x(\text{P}_2\text{O}_5)_{(1-x)}$  glasses are known to show pronounced long-wavelength acoustic-mode softening, their lanthanum  $(\text{La}_2\text{O}_3)_x(\text{P}_2\text{O}_5)_{(1-x)}$  analogues do not. To investigate experimentally this different influence of lanthanide modifiers, a comparative study has been made of the effects of temperature and pressure on the velocities of ultrasonic waves propagated in binary  $((\text{La}_2\text{O}_3)_x(\text{P}_2\text{O}_5)_{(1-x)})$  and  $(\text{Sm}_2\text{O}_3)_x(\text{P}_2\text{O}_5)_{(1-x)}$  and ternary  $((\text{La}_2\text{O}_3)_x(\text{Sm}_2\text{O}_3)_y(\text{P}_2\text{O}_5)_{(1-x-y)})$  phosphate glasses with compositions near to that corresponding to the metaphosphate  $(\text{R}_2\text{O}_3)_{0.25}(\text{P}_2\text{O}_5)_{0.75}$ . For each glass the second-order elastic stiffness tensor components  $C_{ij}^S$  continue to increase down to 10 K in a manner consistent with ultrasonic interactions with two-level systems. Measurements of the effects of hydrostatic pressure on the ultrasonic wave velocities have been used to determine the hydrostatic pressure derivatives  $(\partial C_{ij}^S/\partial P)_{T,P=0}$  of the second-order elastic stiffness tensor components and  $(\partial B_0^S/\partial P)_{T,P=0}$  of the bulk modulus  $B_0^S$  at room temperature (293 K). For the ternary glasses  $(\partial C_{11}^S/\partial P)_{T,P=0}$ ,  $(\partial C_{44}^S/\partial P)_{T,P=0}$  and  $(\partial B_0^S/\partial P)_{T,P=0}$  are small but positive; these glasses stiffen under pressure. Replacement of samarium by lanthanum in the ternary glasses negates the acoustic-mode softening. Possible sources of the different effects of lanthanum and samarium modifiers on the non-linear acoustic properties of metaphosphate glasses are discussed.

## 1. Introduction

The binary rare-earth phosphate glasses containing lanthanum  $(\text{La}_2\text{O}_3)_x(\text{P}_2\text{O}_5)_{1-x}$  [1, 2] and samarium  $(\text{Sm}_2\text{O}_3)_x(\text{P}_2\text{O}_5)_{1-x}$  [1–7] exhibit interesting differences in their non-linear acoustic properties. The lanthanum phosphate glasses show normal behaviour, namely that the application of hydrostatic pressure increases the ultrasonic wave velocities—the usual elastic response to pressure. By contrast the samarium phosphate glasses show an anomalous elastic behaviour under pressure; the hydrostatic pressure derivatives  $(\partial C_{11}^S/\partial P)_{T,P=0}$  and  $(\partial C_{44}^S/\partial P)_{T,P=0}$  of the elastic stiffnesses are negative: the long-wavelength acoustic-mode Grüneisen parameters  $\gamma_L$  and  $\gamma_S$  are negative. Hence the long-wavelength acoustic phonons soften under pressure. As a consequence, the samarium phosphate glasses have a negative hydrostatic pressure derivative  $(\partial B_0^S/\partial P)_{T,P=0}$  of the adiabatic bulk modulus  $B_0^S$ : when subjected to high pressures, they have the remarkable property of becoming easier to squeeze. It is our present aim to compare the elastic behaviour of ternary phosphate glasses  $(\text{La}_2\text{O}_3)_x(\text{Sm}_2\text{O}_3)_y(\text{P}_2\text{O}_5)_{(1-x-y)}$  containing both lanthanum and samarium as network modifiers with those of the binary  $(\text{La}_2\text{O}_3)_x(\text{P}_2\text{O}_5)_{1-x}$  and  $(\text{Sm}_2\text{O}_3)_x(\text{P}_2\text{O}_5)_{1-x}$  glasses. The glasses studied have a composition close to that of metaphosphate  $\text{R}(\text{PO}_3)_3$ , where R corresponds to La or Sm. The object has been to find out whether the elastic properties under temperature and pressure change systematically when

lanthanum replaces samarium. To achieve this, the longitudinal and shear ultrasonic wave velocities of the glasses have been measured from 10 K to 350 K. The changes in the ultrasonic wave velocity induced by application of hydrostatic pressure up to 0.15 GPa have also been measured at room temperature. The experimental results provide details of the temperature dependences of the second-order elastic stiffness tensor components (SOECs) and the hydrostatic pressure derivatives of the elastic stiffnesses and bulk modulus.

The SOECs and their hydrostatic pressure derivatives have been used to determine the long-wavelength acoustic-mode Grüneisen parameters which quantify the first-order terms of the vibrational anharmonicity of the long-wavelength acoustic phonon modes, i.e. the non-linearity of the atomic forces with respect to atomic displacements. Physical properties such as the temperature dependence of the SOECs, which are governed by thermal motion, depend upon vibrational anharmonicity. The present work provides a quantitative description of the vibrational anharmonicity of the long-wavelength acoustic phonons of these binary and ternary lanthanum and samarium phosphate glasses.

## 2. Experimental procedure

Phosphate glasses of the types  $(\text{La}_2\text{O}_3)_x(\text{Sm}_2\text{O}_3)_y(\text{P}_2\text{O}_5)_{(1-x-y)}$ ,  $(\text{La}_2\text{O}_3)_x(\text{P}_2\text{O}_5)_{(1-x)}$  and  $(\text{Sm}_2\text{O}_3)_x$

(P<sub>2</sub>O<sub>5</sub>)<sub>(1-x)</sub> were manufactured from laboratory reagent 99.9% purity grades of phosphorus pentoxide P<sub>2</sub>O<sub>5</sub>, lanthanum oxide La<sub>2</sub>O<sub>3</sub> and samarium oxide Sm<sub>2</sub>O<sub>3</sub>. The oxides were mixed together in quantities of about 25 g and then heated for one hour at 500 °C in a covered alumina crucible inside an electric furnace. The mixture was then melted in a second furnace and held for a further hour at 1350 °C. The molten mixture was quenched rapidly into a preheated (500 °C) steel split mould to make up a glass cylinder approximately 10 mm long and 14 mm in diameter. After casting, the glass was transferred immediately to an annealing furnace at 500 °C for 24 h. After this the furnace was switched off and the glass allowed to cool down to room temperature at a rate of 0.5 °C min<sup>-1</sup>.

The glasses prepared using this technique are transparent and of optical quality; the ones containing samarium are yellow in colour. The compositions of the glass samples were determined by quantitative analysis using a Jeol JXA-8600M electron probe microanalyser (EPMA) fitted with wavelength-dispersive spectrometers (WDS). The microanalyser was fitted with four double-crystal spectrometers which could be used to analyse the X-ray spectrum of the elements present. Pure samples of SmS and LaP<sub>5</sub>O<sub>14</sub> were used as a standard. Using this technique, the electron beam could be directed at a relatively small area without destroying the sample. The chemical compositions are given in Table I. The density was measured at room temperature and atmospheric pressure by Archimedes' method using toluene as a flotation fluid.

Samples were cut and polished to have flat and parallel faces to within 10<sup>-3</sup> rad and to have a thickness of about 6 mm, suitable for ultrasonic wave velocity measurements. Parallelism of the faces was

examined using an optical interference method and confined to within one wavelength of sodium light. To carry out the ultrasonic experiments, quartz transducers (X-cut for longitudinal; Y-cut for shear waves), driven at their fundamental frequency of 10 MHz, were bonded to the specimens. For determination of the temperature dependences of the SOECs in the low-temperature region, Nonaq stopcock grease was used as the bonding agent between samples and transducers; Dow Resin 276-V9 was employed above room temperature.

The ultrasonic wave velocities were measured from 10 to 350 K using the pulse echo overlap technique [8], which has a sensitivity of better than 1 part in 10<sup>5</sup>. The sample was placed in a closed-cycle helium cryostat and the temperature monitored using a temperature sensor. The temperature was recorded (to better than ± 0.1 K) with the aid of a digital multimeter. The pulse echo overlap technique was also used to determine the changes in ultrasonic wave velocity under hydrostatic pressure up to 0.15 GPa, over which range a linear dependence was found. The hydrostatic pressure was applied in a piston-and-cylinder apparatus using silicone oil as the pressure-transmitting medium. The pressure was determined from the change in resistance of a precalibrated manganin wire coil in the pressure cell.

### 3. Results

#### 3.1. Temperature dependences of SOECs

The longitudinal ( $v_L$ ) and shear ( $v_S$ ) ultrasonic wave velocities, and hence the two independent adiabatic SOECs, as well as related physical properties, calculated from the experimental data obtained at room temperature, for each glass are given in Table I.

TABLE I Comparison of the acoustic properties at room temperature (293 K) of ternary (La<sub>2</sub>O<sub>3</sub>)<sub>x</sub>(Sm<sub>2</sub>O<sub>3</sub>)<sub>y</sub>(P<sub>2</sub>O<sub>5</sub>)<sub>(1-x-y)</sub> glasses with those of the binary phosphate (La<sub>2</sub>O<sub>3</sub>)<sub>x</sub>(P<sub>2</sub>O<sub>5</sub>)<sub>(1-x)</sub> and (Sm<sub>2</sub>O<sub>3</sub>)<sub>x</sub>(P<sub>2</sub>O<sub>5</sub>)<sub>(1-x)</sub> glasses

| Property                                       | (La <sub>2</sub> O <sub>3</sub> ) <sub>x</sub> (Sm <sub>2</sub> O <sub>3</sub> ) <sub>y</sub> (P <sub>2</sub> O <sub>5</sub> ) <sub>(1-x-y)</sub> |                         | (La <sub>2</sub> O <sub>3</sub> ) <sub>x</sub> (P <sub>2</sub> O <sub>5</sub> ) <sub>(1-x)</sub> |           | (Sm <sub>2</sub> O <sub>3</sub> ) <sub>x</sub> (P <sub>2</sub> O <sub>5</sub> ) <sub>(1-x)</sub> |           |
|--|---|-------------------------|--|-----------|--|-----------|
|  | x = 0.055,<br>y = 0.206   | x = 0.166,<br>y = 0.086 | x = 0.222  | x = 0.263 | x = 0.212  | x = 0.224 |
| Density (kg m <sup>-3</sup> )                  | 3505  | 3569                    | 3346   | 3413      | 3271   | 3280      |
| Ultrasonic wave velocities (m <sup>-1</sup> s) |   |                         |  |           |  |           |
| $v_L$  | 4582  | 4630                    | 4428   | 4451      | 4516   | 4500      |
| $v_S$  | 2608  | 2631                    | 2491   | 2599      | 2674   | 2684      |
| Elastic stiffnesses (GPa)                      |   |                         |  |           |  |           |
| $C_{11}^S$                                     | 73.7  | 76.5                    | 65.9   | 67.6      | 66.7   | 66.4      |
| $C_{44}^S$                                     | 23.8  | 24.7                    | 20.8   | 23.1      | 23.4   | 23.6      |
| Elastic moduli (GPa)                           |   |                         |  |           |  |           |
| $B_0^S$  | 41.9  | 46.6                    | 38.2   | 36.9      | 35.9   | 34.9      |
| $E^S$  | 60.1  | 62.3                    | 52.7   | 57.2      | 57.7   | 57.8      |
| $\sigma^S$                                     | 0.261   | 0.262                   | 0.270  | 0.241     | 0.230  | 0.224     |
| Pressure derivatives                           |   |                         |  |           |  |           |
| $(\partial C_{11}^S / \partial P)_{P=0}$       | 0.08  | 1.50                    | 2.19   | 3.56      | -1.31  | -1.09     |
| $(\partial C_{44}^S / \partial P)_{P=0}$       | 0.02  | 0.06                    | 0.11   | 0.13      | -0.67  | -0.72     |
| $(\partial B_0^S / \partial P)_{P=0}$          | 0.05  | 1.43                    | 2.04   | 3.39      | -0.41  | -0.13     |
| Grüneisen parameters                           |   |                         |  |           |  |           |
| $\gamma_L$                                     | -0.14   | 0.26                    | 0.47   | 0.80      | -0.51  | -0.45     |
| $\gamma_S$                                     | -0.15   | -0.12                   | -0.06  | -0.06     | -0.68  | -0.70     |
| $\gamma^{el}$                                  | -0.15   | 0.01                    | 0.11   | 0.23      | -0.67  | -0.62     |

The behaviours with temperature of the second-order elastic stiffnesses  $C_{IJ}^S$  of the ternary  $(\text{La}_2\text{O}_3)_{0.055}(\text{Sm}_2\text{O}_3)_{0.206}(\text{P}_2\text{O}_5)_{0.739}$  and  $(\text{La}_2\text{O}_3)_{0.166}(\text{Sm}_2\text{O}_3)_{0.086}(\text{P}_2\text{O}_5)_{0.748}$  glasses are given Tables II and III. Both  $C_{11}^S$  and  $C_{44}^S$  increase down to low temperatures. There are small anomalies just below room temperature; these are similar, although less pronounced, to those observed previously for samarium phosphate glasses, for which there is a temperature region in which the modulus decreases with temperature [7]; this behaviour has been attributed to acoustic phonon-mode softening. The ultrasonic wave velocities of the lanthanum phosphate glasses increase linearly in the more usual fashion as the temperature is reduced [3]. Below 100 K the elastic stiffnesses of the  $(\text{La}_2\text{O}_3)_x(\text{Sm}_2\text{O}_3)_y(\text{P}_2\text{O}_5)_{(1-x-y)}$  glasses show progressively larger increases as the temperature is decreased. This behaviour, which has also been observed in samarium phosphate glasses [7], is consistent with the ultrasonic phonons interacting with two-level systems.

### 3.2. Hydrostatic pressure derivatives of SOECs

The hydrostatic pressure derivatives of the SOECs were obtained using the following expressions:

$$\left(\frac{\partial C_{11}}{\partial P}\right)_{T, P=0} = 2C_{11} \left(\frac{d[(W_L/W_{L0}) - 1]}{dP}\right)_{T, P=0} + \frac{C_{11}}{3B^S} \quad (1)$$

$$\left(\frac{\partial C_{44}}{\partial P}\right)_{T, P=0} = 2C_{44} \left(\frac{d[(W_S/W_{S0}) - 1]}{dP}\right)_{T, P=0} + \frac{C_{44}}{3B^S} \quad (2)$$

$$\left(\frac{\partial B}{\partial P}\right)_{T, P=0} = \frac{2}{3} \left( 3C_{11} \frac{d[(W_L/W_{L0}) - 1]}{dP} - 4C_{44} \frac{d[(W_S/W_{S0}) - 1]}{dP} \right)_{T, P=0} \quad (3)$$

where  $W$  and  $W_0$  are the natural velocity [9] and its zero pressure value, respectively, and  $L$  and  $S$  refer to longitudinal and shear ultrasonic modes, respectively. The changes induced by hydrostatic pressure at room temperature on the natural velocity  $((W/W_0) - 1)$  of longitudinal and shear ultrasonic waves propagated in  $(\text{La}_2\text{O}_3)_x(\text{Sm}_2\text{O}_3)_y(\text{P}_2\text{O}_5)_{(1-x-y)}$  glasses are given in Fig. 1. The data show that these ternary glasses display pressure dependences intermediate between those of the binary lanthanum and samarium phosphate glasses. The hydrostatic pressure derivative  $(\partial C_{11}^S/\partial P)_{T, P=0}$  of both  $(\text{La}_2\text{O}_3)_x(\text{Sm}_2\text{O}_3)_y(\text{P}_2\text{O}_5)_{(1-x-y)}$

TABLE II Temperature dependences of longitudinal ( $v_L$ ) and shear ( $v_S$ ) ultrasonic wave velocities and adiabatic elastic stiffnesses  $C_{11}^S$  and  $C_{44}^S$ , together with the technical elastic moduli: bulk modulus  $B^S$ , Young's modulus  $E^S$  and Poisson's ratio  $\sigma^S$  of  $(\text{La}_2\text{O}_3)_{0.166}(\text{Sm}_2\text{O}_3)_{0.086}(\text{P}_2\text{O}_5)_{0.748}$  glass; estimated experimental errors  $C_{11}^S \pm 0.1$ ,  $C_{44}^S \pm 0.2$ ,  $B^S \pm 0.4$ ,  $E^S \pm 0.4$  and  $\sigma^S \pm 0.002$

| $T$<br>(K) | $v_L$<br>( $\text{m s}^{-1}$ ) | $v_S$<br>( $\text{m s}^{-1}$ ) | $C_{11}^S$<br>(GPa) | $C_{44}^S$<br>(GPa) | $B_0^S$<br>(GPa) | $E^S$<br>(GPa) | $\sigma^S$ |
|------------|--------------------------------|--------------------------------|---------------------|---------------------|------------------|----------------|------------|
| 10         | 4669                           | 2663                           | 77.8                | 25.3                | 44.1             | 63.7           | 0.259      |
| 20         | 4666                           | 2662                           | 77.7                | 25.3                | 44.0             | 63.7           | 0.259      |
| 30         | 4663                           | 2660                           | 77.6                | 25.3                | 43.9             | 63.6           | 0.259      |
| 40         | 4661                           | 2658                           | 77.5                | 25.2                | 43.9             | 63.5           | 0.259      |
| 50         | 4658                           | 2657                           | 77.4                | 25.2                | 43.8             | 63.4           | 0.259      |
| 60         | 4655                           | 2655                           | 77.3                | 25.2                | 43.8             | 63.4           | 0.259      |
| 70         | 4653                           | 2654                           | 77.3                | 25.1                | 43.8             | 63.3           | 0.259      |
| 80         | 4650                           | 2652                           | 77.2                | 25.1                | 43.7             | 63.2           | 0.259      |
| 90         | 4649                           | 2651                           | 77.1                | 25.1                | 43.7             | 63.2           | 0.259      |
| 100        | 4648                           | 2650                           | 77.1                | 25.1                | 43.7             | 63.1           | 0.259      |
| 110        | 4645                           | 2649                           | 77.0                | 25.0                | 43.6             | 63.1           | 0.259      |
| 120        | 4644                           | 2646                           | 77.0                | 25.0                | 43.7             | 63.0           | 0.260      |
| 130        | 4643                           | 2645                           | 77.0                | 25.0                | 43.7             | 63.0           | 0.260      |
| 140        | 4642                           | 2644                           | 76.9                | 25.0                | 43.7             | 62.9           | 0.260      |
| 150        | 4641                           | 2643                           | 76.9                | 24.9                | 43.6             | 62.8           | 0.260      |
| 160        | 4640                           | 2642                           | 76.8                | 24.9                | 43.6             | 62.8           | 0.260      |
| 170        | 4639                           | 2641                           | 76.8                | 24.9                | 43.6             | 62.7           | 0.260      |
| 180        | 4638                           | 2640                           | 76.8                | 24.9                | 43.6             | 62.7           | 0.260      |
| 190        | 4636                           | 2639                           | 76.7                | 24.9                | 43.6             | 62.7           | 0.260      |
| 200        | 4635                           | 2637                           | 76.7                | 24.8                | 43.6             | 62.6           | 0.261      |
| 210        | 4634                           | 2636                           | 76.7                | 24.8                | 43.6             | 62.6           | 0.261      |
| 220        | 4632                           | 2635                           | 76.6                | 24.8                | 43.5             | 62.5           | 0.261      |
| 230        | 4631                           | 2634                           | 76.5                | 24.8                | 43.5             | 62.5           | 0.261      |
| 240        | 4630                           | 2633                           | 76.5                | 24.7                | 43.5             | 62.4           | 0.261      |
| 250        | 4629                           | 2632                           | 76.5                | 24.7                | 43.5             | 62.4           | 0.261      |
| 260        | 4628                           | 2631                           | 76.4                | 24.7                | 43.5             | 62.3           | 0.261      |
| 270        | 4627                           | 2631                           | 76.4                | 24.7                | 43.5             | 62.3           | 0.261      |
| 280        | 4626                           | 2630                           | 76.4                | 24.7                | 43.5             | 62.3           | 0.261      |
| 290        | 4626                           | 2629                           | 76.4                | 24.7                | 43.5             | 62.2           | 0.262      |
| 300        | 4626                           | 2628                           | 76.4                | 24.6                | 43.5             | 62.2           | 0.262      |
| 310        | 4627                           | 2627                           | 76.4                | 24.6                | 43.6             | 62.2           | 0.262      |
| 320        | 4627                           | 2626                           | 76.4                | 24.6                | 43.6             | 62.1           | 0.262      |
| 330        | 4626                           | 2625                           | 76.4                | 24.6                | 43.6             | 62.1           | 0.263      |
| 340        | 4625                           | 2623                           | 76.4                | 24.6                | 43.6             | 62.0           | 0.263      |
| 350        | 4625                           | 2622                           | 76.3                | 24.5                | 43.6             | 62.0           | 0.263      |

TABLE III Temperature dependences of longitudinal ( $v_L$ ) and shear ( $v_S$ ) ultrasonic wave velocities and adiabatic elastic stiffnesses  $C_{11}^S$  and  $C_{44}^S$ , together with the technical elastic moduli: bulk modulus  $B^S$ , Young's modulus  $E^S$  and Poisson's ratio  $\sigma^S$  of  $(La_2O_3)_{0.055}(Sm_2O_3)_{0.206}(P_2O_5)_{0.739}$  glass; estimated experimental errors  $C_{11}^S \pm 0.1$ ,  $C_{44}^S \pm 0.2$ ,  $B^S \pm 0.4$ ,  $E^S \pm 0.4$  and  $\sigma^S \pm 0.002$

| $T$<br>(K) | $v_L$<br>( $m s^{-1}$ ) | $v_S$<br>( $m s^{-1}$ ) | $C_{11}^S$<br>(GPa) | $C_{44}^S$<br>(GPa) | $B_0^S$<br>(GPa) | $E^S$<br>(GPa) | $\sigma^S$ |
|------------|-------------------------|-------------------------|---------------------|---------------------|------------------|----------------|------------|
| 10         | 4613                    | 2638                    | 74.6                | 24.4                | 42.1             | 61.3           | 0.257      |
| 20         | 4611                    | 2636                    | 74.5                | 24.4                | 42.1             | 61.3           | 0.257      |
| 30         | 4609                    | 2634                    | 74.5                | 24.3                | 42.0             | 61.2           | 0.258      |
| 40         | 4607                    | 2633                    | 74.4                | 24.3                | 42.0             | 61.1           | 0.258      |
| 50         | 4606                    | 2631                    | 74.4                | 24.3                | 42.0             | 61.0           | 0.258      |
| 60         | 4604                    | 2629                    | 74.3                | 24.2                | 42.0             | 61.0           | 0.258      |
| 70         | 4602                    | 2628                    | 74.3                | 24.2                | 42.0             | 60.9           | 0.258      |
| 80         | 4601                    | 2627                    | 74.2                | 24.2                | 42.0             | 60.9           | 0.258      |
| 90         | 4600                    | 2625                    | 74.2                | 24.2                | 42.0             | 60.8           | 0.259      |
| 100        | 4599                    | 2624                    | 74.2                | 24.1                | 42.0             | 60.8           | 0.259      |
| 110        | 4598                    | 2623                    | 74.1                | 24.1                | 42.0             | 60.7           | 0.259      |
| 120        | 4597                    | 2622                    | 74.1                | 24.1                | 42.0             | 60.7           | 0.259      |
| 130        | 4596                    | 2621                    | 74.1                | 24.1                | 42.0             | 60.6           | 0.259      |
| 140        | 4596                    | 2620                    | 74.1                | 24.1                | 42.0             | 60.6           | 0.259      |
| 150        | 4595                    | 2619                    | 74.0                | 24.0                | 42.0             | 60.6           | 0.259      |
| 160        | 4594                    | 2618                    | 74.0                | 24.0                | 42.0             | 60.5           | 0.260      |
| 170        | 4593                    | 2618                    | 74.0                | 24.0                | 41.9             | 60.5           | 0.259      |
| 180        | 4593                    | 2617                    | 74.0                | 24.0                | 41.9             | 60.5           | 0.260      |
| 190        | 4592                    | 2616                    | 73.9                | 24.0                | 41.9             | 60.5           | 0.260      |
| 200        | 4591                    | 2615                    | 73.9                | 24.0                | 41.9             | 60.4           | 0.260      |
| 210        | 4591                    | 2614                    | 73.9                | 24.0                | 41.9             | 60.4           | 0.260      |
| 220        | 4590                    | 2613                    | 73.9                | 23.9                | 41.9             | 60.3           | 0.260      |
| 230        | 4589                    | 2612                    | 73.8                | 23.9                | 41.9             | 60.3           | 0.260      |
| 240        | 4588                    | 2611                    | 73.8                | 23.9                | 41.9             | 60.3           | 0.260      |
| 250        | 4588                    | 2610                    | 73.8                | 23.9                | 41.9             | 60.2           | 0.261      |
| 260        | 4587                    | 2610                    | 73.8                | 23.9                | 41.9             | 60.2           | 0.261      |
| 270        | 4586                    | 2609                    | 73.7                | 23.9                | 41.9             | 60.2           | 0.261      |
| 280        | 4585                    | 2608                    | 73.7                | 23.8                | 41.9             | 60.1           | 0.261      |
| 290        | 4585                    | 2608                    | 73.7                | 23.8                | 41.9             | 60.1           | 0.261      |
| 300        | 4584                    | 2607                    | 73.7                | 23.8                | 41.9             | 60.1           | 0.261      |
| 310        | 4583                    | 2606                    | 73.6                | 23.8                | 41.9             | 60.1           | 0.261      |
| 320        | 4582                    | 2605                    | 73.6                | 23.8                | 41.9             | 60.0           | 0.261      |
| 330        | 4581                    | 2605                    | 73.6                | 23.8                | 41.9             | 60.0           | 0.261      |
| 340        | 4580                    | 2604                    | 73.5                | 23.8                | 41.8             | 60.0           | 0.261      |
| 350        | 4579                    | 2604                    | 73.5                | 23.8                | 41.8             | 60.0           | 0.261      |

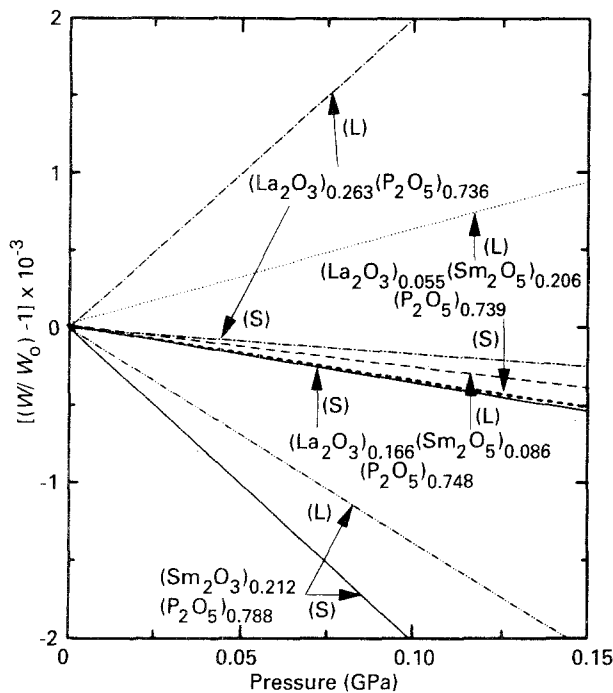


Figure 1 Hydrostatic pressure dependences of the relative change of the natural wave velocity,  $(w/w_0)^{-1}$ , of two ternary glasses at 293 K, compared with those of lanthanum phosphate glasses and samarium phosphate glasses.

glasses are positive. Similar behaviour is shown by the lanthanum phosphate glasses (Table I). In contrast, the pressure derivatives  $(\partial C_{11}^S/\partial P)_{T,P=0}$  and  $(\partial C_{44}^S/\partial P)_{T,P=0}$  of samarium phosphate glasses are negative, with  $(\partial C_{11}^S/\partial P)_{T,P=0}$  being much greater than  $(\partial C_{44}^S/\partial P)_{T,P=0}$  (Table I). The observed pressure dependence is greater for the longitudinal velocity than for the shear mode: there is a volume rather than a shear effect. An instructive result is that in ternary  $(La_2O_3)_{0.055}(Sm_2O_3)_{0.206}(P_2O_5)_{0.739}$  and  $(La_2O_3)_{0.166}(Sm_2O_3)_{0.086}(P_2O_5)_{0.748}$  glasses both  $(\partial C_{11}^S/\partial P)_{T,P=0}$  and  $(\partial B_0^S/\partial P)_{T,P=0}$  have positive values. Unlike the samarium phosphate glasses,  $(La_2O_3)_x(Sm_2O_3)_y(P_2O_5)_{(1-x-y)}$  stiffen in the normal manner under pressure. The bulk modulus, which is to first order in pressure  $P$ , is given by

$$B^T(P) = B_0^T + P(\partial B^S/\partial P)_{T,P=0} \quad (4)$$

and becomes larger as the pressure is increased. The ternary  $(La_2O_3)_{0.055}(Sm_2O_3)_{0.206}(P_2O_5)_{0.739}$  and  $(La_2O_3)_{0.166}(Sm_2O_3)_{0.086}(P_2O_5)_{0.748}$ , like the  $(La_2O_3)_x(P_2O_5)_{(1-x)}$  glasses but in sharp distinction from the  $(Sm_2O_3)_x(P_2O_5)_{(1-x)}$  glasses, become harder to squeeze under pressure in the more usual way.

### 3.3. Compression behaviour

The use of an equation of state allows an estimation of the compression of a material at very high pressures from a knowledge of the isothermal bulk modulus and its hydrostatic pressure derivatives. The calculation of the compression in these glasses has been carried out using the Murnaghan equation of state in its logarithmic form [10]:

$$\ln\left(\frac{V_0}{V}\right) = \frac{1}{B_0'} \ln\left[B_0' \left(\frac{P}{B_0'}\right) + 1\right] \quad (5)$$

which assumes that the bulk modulus depends linearly on pressure (Equation 4). The compressions  $V(P)/V_0$  of the lanthanum–samarium phosphate glasses at 293 K are compared with those for lanthanum and samarium phosphate glasses in Fig. 2. At comparatively low pressures the compressions of all these phosphate glasses are similar, but they diverge with increasing pressure due to the different signs of  $(\partial B_0^S/\partial P)_{T,P=0}$  (Table I). When the pressure is increased, the compression curve of the  $(\text{La}_2\text{O}_3)_{0.055}(\text{Sm}_2\text{O}_3)_{0.206}(\text{P}_2\text{O}_5)_{0.739}$  and  $(\text{La}_2\text{O}_3)_{0.166}(\text{Sm}_2\text{O}_3)_{0.086}(\text{P}_2\text{O}_5)_{0.748}$  glasses with a positive  $(\partial B_0^S/\partial P)_{T,P=0}$  is higher than that for samarium phosphate glass with its negative  $(\partial B_0^S/\partial P)_{T,P=0}$ .

### 3.4. Acoustic-mode Grüneisen parameters and vibrational anharmonicity

The acoustic-mode Grüneisen parameters, which express the volume (or strain) dependences of the normal mode frequency  $\omega_i$ , are given by

$$\gamma_i = \frac{-d(\ln \omega_i)}{d(\ln V)} \quad (6)$$

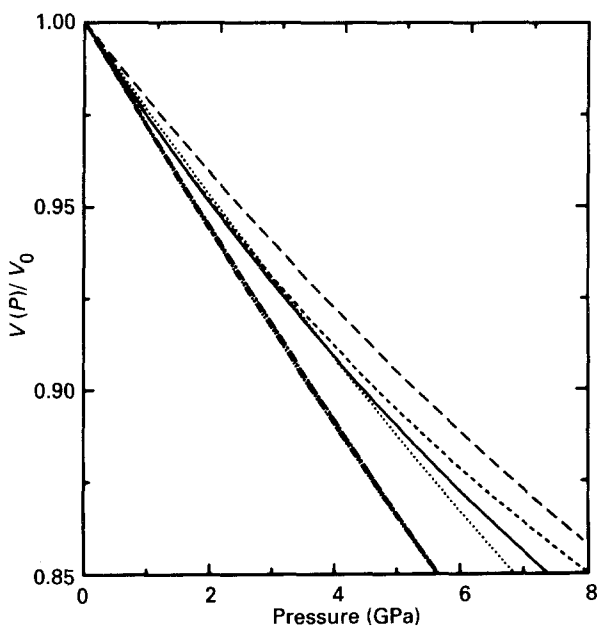


Figure 2 Compression  $V/V_0$  of  $(\cdots)$   $(\text{La}_2\text{O}_3)_{0.055}(\text{Sm}_2\text{O}_3)_{0.206}(\text{P}_2\text{O}_5)_{0.739}$  and  $(\text{---})$   $(\text{La}_2\text{O}_3)_{0.166}(\text{Sm}_2\text{O}_3)_{0.086}(\text{P}_2\text{O}_5)_{0.748}$  glasses at 293 K calculated on the basis of Murnaghan's equation of state, compared with those of  $(\text{---})$   $(\text{La}_2\text{O}_3)_{0.222}(\text{P}_2\text{O}_5)_{0.778}$ ,  $(\text{---})$   $(\text{La}_2\text{O}_3)_{0.263}(\text{P}_2\text{O}_5)_{0.737}$ ,  $(\text{---})$   $(\text{Sm}_2\text{O}_3)_{0.212}(\text{P}_2\text{O}_5)_{0.778}$  and  $(\text{---})$   $(\text{Sm}_2\text{O}_3)_{0.224}(\text{P}_2\text{O}_5)_{0.776}$ .

The present results (Table I) can be used to determine the longitudinal  $\gamma_L$  and shear  $\gamma_S$  acoustic-mode Grüneisen parameters in the long-wavelength limit. Calculated values of the longitudinal  $\gamma_L$  and shear  $\gamma_S$ , together with the mean long-wavelength acoustic-mode Grüneisen parameter

$$\gamma^{\text{el}} = \frac{\gamma_L + 2\gamma_S}{3} \quad (7)$$

of the  $(\text{La}_2\text{O}_3)_{0.055}(\text{Sm}_2\text{O}_3)_{0.206}(\text{P}_2\text{O}_5)_{0.739}$  and  $(\text{La}_2\text{O}_3)_{0.166}(\text{Sm}_2\text{O}_3)_{0.086}(\text{P}_2\text{O}_5)_{0.748}$  glasses at room temperature, are compared with those of the binary phosphate glasses in Table I. The acoustic-mode Grüneisen parameters are negative for the samarium phosphate glasses: application of pressure causes the long-wavelength acoustic-mode frequencies and energies associated with these modes to decrease [1, 2]. In contrast, the long-wavelength acoustic-mode Grüneisen parameters for the lanthanum phosphate glasses show normal behaviour in being positive [1, 2]. Replacement of samarium by lanthanum in the ternary  $(\text{La}_2\text{O}_3)_x(\text{Sm}_2\text{O}_3)_y(\text{P}_2\text{O}_5)_{(1-x-y)}$  glasses results in an intermediate situation between those of the binary glasses: the longitudinal  $\gamma_L$  and shear  $\gamma_S$  mode Grüneisen parameters are shifted in the positive direction. The replacement of samarium by lanthanum cancels the mode-softening effect of samarium. The reason for this difference between the influences of lanthanum and samarium ions is not clear. The major chemical difference between them is that while lanthanum has an exclusively trivalent ion state  $\text{La}^{3+}$ , samarium can exist as either  $\text{Sm}^{3+}$  or the much larger  $\text{Sm}^{2+}$ .

Application of pressure to divalent samarium crystalline compounds can induce a transition via an intermediate valence state towards a trivalent state [11]. An example is  $\text{SmS}$ . The transition from the electronic configuration  $4f^65d^0$  to time-sharing with  $4f^55d^1$  involves a marked size reduction of the samarium ions and as a result crystalline  $\text{SmS}$  shows the unusual decrease of elastic stiffness under pressure [12]. Hence it was surmised [1, 2] that one explanation (among others) of the anomalous elastic behaviour of the samarium phosphate glasses could be that the samarium ions are in a mixed valent state and that under pressure the  $2+$  component is reduced at the expense of  $3+$ , so that the ions occupy a smaller volume with a consequent reduction in elastic stiffness. At first sight it could be salient that the elastic properties of europium phosphate glasses [13] show anomalies similar to those reported for the samarium phosphate glasses. Europium also occurs in either a divalent ( $4f^75s^2-^8\text{S}_{7/2}$ ) or trivalent ( $4f^65s^2-^7\text{F}_0$ ) state: its compounds can also show valence instabilities associated with  $\text{Eu}^{2+}$  and  $\text{Eu}^{3+}$  states. Neodymium phosphate glasses show a normal elastic response to pressure [14]. Lanthanum and neodymium are exclusively trivalent. However, negative pressure dependences of the SOECs and the positive third-order components (TOECs) are not restricted to the glasses containing variable-valence rare-earth ions: pressure-induced acoustic-mode softening has recently been observed in gadolinium metaphosphate glasses [15],

although the effects are much smaller than in the samarium and europium phosphates. To examine their valence state, fluorescence studies of samarium [16] and europium [13] phosphate glasses have been made. In both cases the spectra show that the divalent ion is absent, or at most in very small concentration—not enough to produce the observed large elastic anomalies.

Another possibility is that differences in glass structure could cause the differences in non-linear acoustic properties of the phosphate glasses containing  $\text{La}^{3+}$  or  $\text{Sm}^{3+}$  ions as network modifiers. Structural differences are not expected to be great because the Raman spectra of the two glass types are very similar [1, 2] and furthermore the ion sizes of  $\text{La}^{3+}$  and  $\text{Sm}^{3+}$  are the same (0.104 nm). An indication that there indeed are subtle differences in structure comes from the observation (Table I) that the densities of glasses containing  $\text{La}^{3+}$  tend to be slightly higher than for those containing the same composition of  $\text{Sm}^{3+}$ , even though  $\text{La}^{3+}$  is lighter than  $\text{Sm}^{3+}$ . Phosphate glasses are built up from  $\text{PO}_4$  tetrahedral units in which one oxygen atom is doubly bonded to the phosphorus and does not contribute to the coherence of the network; pairs of  $\text{PO}_4$  tetrahedra can share only one corner. Phosphate glasses having the metaphosphate composition are comprised of long polymeric chains consisting of  $\text{PO}_4$  tetrahedra connected at two corners so that there are two non-bridging oxygen atoms on each tetrahedron [17]. Application of pressure induces similar decreases in the elastic stiffnesses of vitreous  $\text{SiO}_2$  and silica-based glasses [18]. In the case of vitreous  $\text{SiO}_2$ , the pressure-induced acoustic-mode softening effects have been attributed to non-linear acoustic contributions arising from bending vibrations of the bridging oxygen atoms [19]. Another possible microscopic source could be rotations of coupled  $\text{SiO}_4$  tetrahedra which seem to constitute the excess low-frequency harmonic vibrations [20]. In an analogous way non-linear effects of the vibrational modes associated with the corner-linked  $\text{PO}_4$  tetrahedra might be responsible for the elastic anomalies found for phosphate glasses. Thus, either bending vibrations of the bridging oxygen ions or rotations of coupled  $\text{PO}_4$  tetrahedra could be the origin of the acoustic-mode softening under pressure for  $(\text{R}_2\text{O}_3)_x(\text{P}_2\text{O}_5)_{1-x}$  glasses. These vibrations could constitute the additional excitations which recent specific heat measurements have revealed in rare-earth metaphosphate glasses [21].

The universal properties of glasses at very low temperatures can be explained by the phenomenological model of tunnelling in two-level systems [22, 23]. However, above about 1 K, properties such as the plateau in the thermal conductivity and the peak in the temperature dependence of  $C_p/T^3$  cannot be accounted for by the tunnelling model. Additional low-frequency excitations, which co-exist with sound waves, contribute a large excess heat capacity in the temperature range 2 to 20 K [20, 24]. Several conflicting theories have been proposed to explain the anomalous behaviour in this region. One of the more successful and topical phenomenological approaches

is a development of the soft potential model [25, 26] which augments the tunnelling model by a high density of soft anharmonic localized vibrational modes [27–29]. It is feasible that strong anharmonic interactions of acoustic phonons with such localized modes might affect markedly the vibrational anharmonicity of the long-wavelength acoustic waves and hence the higher-order elastic stiffness tensor components. However, the effects of pressure on the elastic behaviour of glasses have not yet been treated in the context of the soft-mode potential model.

#### 4. Conclusions

The elastic and non-linear acoustic properties of ternary  $(\text{La}_2\text{O}_3)_x(\text{Sm}_2\text{O}_3)_y(\text{P}_2\text{O}_5)_{(1-x-y)}$  glasses have been compared with those of the binary  $(\text{Sm}_2\text{O}_3)_x(\text{P}_2\text{O}_5)_{(1-x)}$  and  $(\text{La}_2\text{O}_3)_x(\text{P}_2\text{O}_5)_{(1-x)}$  glasses. The physical significance of the results can be summarized as follows:

1. The anomalous temperature dependences of the ultrasonic wave velocities in the ternary glasses, like those found for  $(\text{Sm}_2\text{O}_3)_x(\text{P}_2\text{O}_5)_{(1-x)}$ , are consistent with interaction of the acoustic phonons with the two-level systems.

2. The hydrostatic pressure derivatives  $(\partial C_{11}^S/\partial P)_{T, P=0}$  and  $(\partial C_{44}^S/\partial P)_{T, P=0}$  and that of the bulk modulus  $(\partial B_0^S/\partial P)_{T, P=0}$  of the  $(\text{La}_2\text{O}_3)_{0.055}(\text{Sm}_2\text{O}_3)_{0.206}(\text{P}_2\text{O}_5)_{0.739}$  and  $(\text{La}_2\text{O}_3)_{0.166}(\text{Sm}_2\text{O}_3)_{0.086}(\text{P}_2\text{O}_5)_{0.748}$  glasses at room temperature are positive. These ternary glasses stiffen under pressure in the normal way like the  $(\text{La}_2\text{O}_3)_x(\text{P}_2\text{O}_5)_{(1-x)}$  glasses.

3. The compressions of the glasses with negative  $(\partial B_0^S/\partial P)_{T, P=0}$  increase much faster under pressure than those with positive  $(\partial B_0^S/\partial P)_{T, P=0}$ .

4. Finally it has been shown that the replacement of samarium by lanthanum in the ternary glasses cancels the acoustic-mode softening effect of samarium.

#### Acknowledgements

We are grateful to Dr S. Bartlett of the Johnson Matthey Technology Centre and to S. Takel of the DRA Maritime Division for their support of this work on rare-earth phosphate glasses. H.B.S. would like to thank the Universiti Pertanian Malaysia and the Government of Malaysia for financial support.

#### References

1. A. MIERZEJEWSKI, G. A. SAUNDERS, H. A. A. SIDEK and B. BRIDGE, *J. Non-Cryst. Solids* **104** (1988) 323.
2. A. MIERZEJEWSKI, G. A. SAUNDERS, H. A. A. SIDEK, R. N. HAMPTON and I. J. AL-MUMMAR, *Solid State Ionics* **28–30** (1988) 778.
3. H. A. A. SIDEK, G. A. SAUNDERS, R. N. HAMPTON, R. C. J. DRAPER and B. BRIDGE, *Phil. Mag. Lett.* **57** (1988) 49.
4. QINGXIAN WANG, G. A. SAUNDERS, E. F. LAMBSON, V. BAYOT and J.-P. MICHENAUND, *J. Non-Cryst. Solids* **125** (1990) 287.
5. G. CARINI, M. CUTRONI, G. D'ANGELO, M. FEDERICO, G. GALLI, G. TRIPODO, G. A. SAUNDERS and Q. WANG, *ibid.* **121** (1990) 288.

6. H. B. SENIN, Q. WANG, G. A. SAUNDERS, R. C. J. DRAPER, H. M. FAROK, M. CANKURTARAN, P. J. FORD, W. POON, H. VASS and B. BRIDGE, in "Developments in Acoustics and Ultrasonics", edited by M. Povey and J. McClements (Institute of Physics, London, 1992) p. 197.
7. H. B. SENIN, Q. WANG, G. A. SAUNDERS and E. F. LAMBSON, *J. Non-Cryst. Solids* **152** (1993) 83.
8. E. P. PAPADAKIS, *J. Acoust. Soc. Amer.* **42** (1967) 1045.
9. R. N. THURSTON and K. BRUGGER, *Phys. Rev.* **133** (1964) A1604.
10. F. D. MURNAGHAN, *Proc. Nat. Acad. Sci.* **30** (1944) 244.
11. A. JAYARAMAN, V. NARAYAMANURTI, E. BUCHER and R. G. MAINES, *Phys. Rev. Lett.* **25** (1970) 1430.
12. TU HAILING, G. A. SAUNDERS and H. BACH, *Phys. Rev. B* **29** (1984) 1848.
13. H. M. FAROK, H. B. SENIN, G. A. SAUNDERS, W. POON and H. VASS, to be published.
14. H. B. SENIN, H. A. A. SIDEK, P. J. FORD, G. A. SAUNDERS, Q. WANG, R. C. J. DRAPER and W. A. LAMBSON, in "Advances in Amorphous State Chemistry" (Society of Glass Technology, Sheffield, 1993) p. 55.
15. H. B. SENIN, G. A. SAUNDERS, LI JIAQIANG and P. J. FORD, to be published.
16. H. M. FAROK, G. A. SAUNDERS, W. POON and H. VASS, *J. Non-Cryst. Solids* **142** (1992) 175.
17. S. W. MARTIN, *Eur. J. Solid State Inorg. Chem.* **28** (1991) 163.
18. E. H. BOGARDUS, *J. Appl. Phys.* **36** (1965) 2504.
19. Y. SATO and O. L. ANDERSON, *J. Phys. Chem. Phys. Solids* **41** (1980) 401.
20. U. BUCHENAU, M. PRAGER, N. NÜCKER, A. J. DIANOUX, N. AHMAD and W. A. PHILLIPS, *Phys. Rev. B* **34** (1986) 5665.
21. G. CARINI, G. D'ANGELO, G. TRIPODO and G. A. SAUNDERS, to be published.
22. P. W. ANDERSON, B. I. HALPERIN and C. M. VARMA, *Phil. Mag.* **25** (1972) 1.
23. W. A. PHILLIPS, *J. Low-Temp. Phys.* **7** (1972) 351.
24. R. O. POHL, in "Amorphous Solids—Low-Temperature Properties", edited by W. A. Phillips (Springer, Berlin, 1981) p. 27.
25. V. G. KARPOV, M. I. KLINGER and F. N. IGNATEV, *Zh. Eksp. Teor. Fiz.* **84** (1983) 760 (*Sov. Phys. JETP* **57** (1983) 439).
26. YU. M. GALPERIN, V. G. KARPOV and V. I. KOZUB, *Adv. Phys.* **38** (1989) 669.
27. U. BUCHENAU, YU. M. GALPERIN, V. L. GUREVICH and H. R. SCHOBBER, *Phys. Rev. B* **43** (1991) 5039.
28. U. BUCHENAU, YU. M. GALPERIN, V. L. GUREVICH, D. A. PARSHIN, M. A. RAMOS and H. R. SCHOBBER, *ibid.* **46** (1992) 2798.
29. L. GIL, M. A. RAMOS, A. BRINGER and U. BUCHENAU, *Phys. Rev. Lett.* **70** (1993) 182.

*Received 29 July  
and accepted 26 August 1993*